

Modelling Steep Terrain Influences on Flow Patterns at the Isle of Helgoland

by U. NIEMEIER and K. H. SCHLÜNZEN

Meteorologisches Institut, Universität Hamburg, Bundesstraße 55, 2000 Hamburg 13, Germany

(Manuscript received September 9, 1992; accepted March 25, 1993)

Abstract

A three-dimensional mesoscale model is used to study the influences of the isle of Helgoland on the wind field around the island. The model simulations are performed for eight different geostrophic wind directions for a neutral atmospheric stratification. These case studies are sufficient to estimate the general influence of the steep coasts of Helgoland on the flow patterns at the island as is shown by the calculation of the characteristic dimensionless numbers.

The simulations are performed with the nonhydrostatic mesoscale model METRAS. It can be applied for terrain slopes up to 70° as is proved by systematic model runs over idealized topography for different terrain slopes. The model results for the small island Helgoland (slopes up to 55°) show that the wind velocity is strongly influenced by the island, much more than the wind direction. The velocity can be enlarged or reduced by more than 50 % for some geostrophic wind directions at several places. The vertical winds show strong upward motions on the windward and downward motions on the lee side of the island. They reach values of about $\pm 2 \text{ ms}^{-1}$ for a geostrophic wind of 4.5 ms^{-1} .

At three sites on the island wind velocity and direction are measured on a routine basis. A fourth site is used for measurement campaigns. The interpretation of the calculated flow patterns for the four wind measurement sites shows the strong mesoscale influences on the wind field. The simulated deviations reach up to 30 % between values for the horizontal wind velocities over the island at the measurement sites and over the undisturbed sea. Only at a model grid point corresponding to the measurement site south pier placed on the island as far away as possible from the "Oberland", the deviations are lower than 10 % for all wind directions. The modelled deviations are used for a correction of the measured data. It is shown that mesoscale influences on the wind field are modelled correctly whereas some local effects are not included in the present model calculations.

Zusammenfassung

Numerische Simulation des Einflusses steilen Geländes auf die Strömungsfelder im Bereich der Insel Helgoland

Mit einem dreidimensionalen mesoskaligen Modell wurde der Einfluß der Insel Helgoland auf das Strömungsfeld untersucht und dazu Modellrechnungen für acht verschiedene Windrichtungen, jeweils bei neutraler Schichtung der Atmosphäre, durchgeführt. Diese Fallstudien reichen aus, um die Einflüsse der steilen Küsten Helgolands auf das regionale Windfeld allgemein abzuschätzen, wie über dimensionslose Kennzahlen belegt wird.

Systematische Simulationen der Strömung um einen idealisierten Berg mit verschiedener Steigung ergaben, daß sich das verwendete nichthydrostatische, mesoskalige Modell METRAS für Geländesteigungen bis zu 70° anwenden läßt. Die modellierten Strömungsfelder im Bereich der kleinen Insel Helgoland (Steigungen bis 55°) zeigen deutlich den Inseleinfluß in der Windgeschwindigkeit, jedoch nur geringe Änderungen in der Windrichtung. An einigen Stellen nimmt die horizontale Windgeschwindigkeit um bis zu 50 % gegenüber den großräumigen Werten zu bzw. ab. An der Luvseite der Insel treten Aufwinde, an der Leeseite Abwinde auf. Der Vertikalwind erreicht bei einer geostrophischen Geschwindigkeit von 4.5 ms^{-1} Werte bis zu $\pm 2 \text{ ms}^{-1}$.

Auf der Insel werden routinemäßig drei Windmäste betrieben, ein vierter wird für Meßkampagnen genutzt. Die Auswertung der simulierten Windfelder in Hinblick auf die vier Meßorte zeigt den mesoskaligen Einfluß der Insel auf das Windfeld. Die Abweichungen von der ungestörten Windgeschwindigkeit über See betragen bis zu 30 %. Nur an dem Modellgitterpunkt, welcher dem am weitesten vom Oberland entfernten Meßmast entspricht (Südmole), liegen die Änderungen bei jeder Windrichtung unter 10 %. Die errechneten Änderungen der Windgeschwindigkeit werden zur Korrektur der Messungen benutzt. Die Ergebnisse zeigen, daß mesoskalige Einflüsse in den Modellrechnungen richtig wiedergegeben werden. Einige lokale Effekte sind dagegen in den vorgestellten Modellrechnungen nicht enthalten.

1 Introduction

Helgoland, an island with steep coasts, is situated about 70 km from the mainland in the German Bight. The rock plateau lies up to 62 m above sea-level, and has a width of a few 100 m and a length of about 1 km. The exposed position of the island in the ocean makes it a favourable place for different kinds of measurements. Not only biological and oceanographic but also meteorological data for the marine environment are collected. The latter are used as input values for weather forecast models, for instance. For this purpose they should be representative of the surrounding maritime area and be influenced as little as possible by local effects. Thus, it is important to find measurement sites on the island where area-representative measurements can be taken, or at least to specify local influences on the measurements. This can be done in two ways:

- A number of measurements can be performed at different sites at and around the island to measure the local influences and to determine the most representative measurement site. To do this successfully, it is necessary to operate several measurement sites for at least one year.
- Alternatively, the flow pattern in the area of the island of interest can be obtained from a mesoscale model which should be able to calculate directly all important local effects. From the model results, local influences at the measurement sites can be inferred. Places with large or low local structures in the flow patterns may be derived and suitable measurement sites determined.

Up to now, only a few models have been used to specify local influences on measurements, the main emphasis being a comparison with measurements or their explanation (e.g. Avissar and Mahrer, 1988; Clark and Gall, 1982; Pielke and Mahrer, 1978; Schumann et al., 1987; Wippermann and Gross, 1981; among others). The intention of the present paper is to infer local influences on measurements from model results.

Here, a mesoscale model is used to simulate the flow patterns at Helgoland. The steep coasts are an essential influence parameter for the calculated wind fields. Thus, the main emphasis in the model description (Section 2) is put on the consideration of steep terrain. The model runs have been initialized with respect to a generalization of the results (Section 3). The wind velocities at the measurement sites are estimated from the calculated flow patterns and compared to measurements (Section 4). Indica-

tions are given for area-representative wind measurement sites at Helgoland and the general validity of the model results is discussed (Section 5).

2 Model Description

The simulations were performed using the non-hydrostatic, three-dimensional mesoscale transport and fluid (stream) model METRAS. It was developed at the Department of Meteorology, University of Hamburg, for the calculation of atmospheric flows in the mesoscale γ - and β -range (Schlünzen, 1990). Additionally it is used for the estimation of atmospheric contaminant inputs to coastal waters (e.g. Schlünzen and Krell, 1993) and for pollution transport studies (Bigalke, 1991; Schlünzen and Pahl, 1992).

2.1 Mesoscale Model

An explicit description of the model is given in Schlünzen (1988, 1990). Here only those features of the model are described in more detail which are important for the present simulations and for the consideration of steep terrain.

The model is based on the fundamental conservation principles of fluid mechanics, namely those of mass, momentum and energy. A terrain-following coordinate-system with the vertical coordinate

$$\eta = z_t \frac{z - z_s(x, y)}{z_t - z_s(x, y)} \quad (1)$$

is applied (see e.g. Pielke, 1984). At the surface (height $z_s(x, y)$ above sea-level) and at the model top (constant height z_t above sea-level) the values of η are zero and z_t respectively. The horizontal cartesian coordinate system is to be rotated against north in any desired angles ζ . In the model calculations of flow patterns at the isle of Helgoland, the rotation of the coordinate system is 45°. The x-axis of the model is thus orientated northeast, the y-axis northwest.

The rotation of the coordinate system and a non-uniform grid structure in vertical as well as in horizontal directions ensure a high resolution of the steep topography. In the model calculations the fine mesh is used in the areas of interest close to the measurement sites and at the cliffs. The rotation of the coordinate system and the non-uniform grid reduce the model requirements on computer resources.

In the model the wind field, temperature, humidity, and tracer concentrations are calculated from prognostic equations, pressure and density from diagnostic ones. As will be shown in Section 3, model simulations with a neutral atmospheric stratification are sufficient for the calculation of representative flow patterns at the isle of Helgoland. The influence of thermodynamic processes may be neglected and only the wind field has to be calculated. Therefore, in the following the model review is restricted to the dynamic part of the model. The prognostic equations for the horizontal components \bar{u} , \bar{v} of the wind vector and the vertical wind \bar{w} are used in the model as follows:

$$\begin{aligned} \frac{\partial \rho_0^* \bar{u}}{\partial t} = & -\frac{\partial}{\partial \dot{x}^1} \{\bar{u}^1 \rho_0^* \bar{u}\} - \frac{\partial}{\partial \dot{x}^2} \{\bar{u}^2 \rho_0^* \bar{u}\} - \\ & - \frac{\partial}{\partial \dot{x}^3} \{\bar{u}^3 \rho_0^* \bar{u}\} - \\ & - \alpha \frac{\partial \dot{x}^1}{\partial x} \left\{ \frac{\partial p_1}{\partial \dot{x}^1} + \frac{\partial p_2}{\partial \dot{x}^1} \right\} - \alpha \frac{\partial \dot{x}^3}{\partial x} \frac{\partial p_2}{\partial \dot{x}^3} + \\ & + \tilde{\rho} \alpha g \frac{\partial \dot{x}^3}{\partial x} \frac{\partial z}{\partial \dot{x}^3} + \\ & + f \{ \rho_0^* \bar{v} - \rho_0^* V_g \} - f' d' \rho_0^* \bar{w} - \bar{F}_1 \end{aligned} \quad (2a)$$

$$\begin{aligned} \frac{\partial \rho_0^* \bar{v}}{\partial t} = & -\frac{\partial}{\partial \dot{x}^1} \{\bar{u}^1 \rho_0^* \bar{v}\} - \frac{\partial}{\partial \dot{x}^2} \{\bar{u}^2 \rho_0^* \bar{v}\} - \\ & - \frac{\partial}{\partial \dot{x}^3} \{\bar{u}^3 \rho_0^* \bar{v}\} - \\ & - \alpha \frac{\partial \dot{x}^2}{\partial y} \left\{ \frac{\partial p_1}{\partial \dot{x}^2} + \frac{\partial p_2}{\partial \dot{x}^2} \right\} - \alpha \frac{\partial \dot{x}^3}{\partial y} \frac{\partial p_2}{\partial \dot{x}^3} + \\ & + \tilde{\rho} \alpha g \frac{\partial \dot{x}^3}{\partial y} \frac{\partial z}{\partial \dot{x}^3} - \\ & - f \{ \rho_0^* \bar{u} - \rho_0^* U_g \} + f' d \rho_0^* \bar{w} - \bar{F}_2 \end{aligned} \quad (2b)$$

$$\begin{aligned} \frac{\partial \rho_0^* \bar{w}}{\partial t} = & -\frac{\partial}{\partial \dot{x}^1} \{\bar{u}^1 \rho_0^* \bar{w}\} - \frac{\partial}{\partial \dot{x}^2} \{\bar{u}^2 \rho_0^* \bar{w}\} - \\ & - \frac{\partial}{\partial \dot{x}^3} \{\bar{u}^3 \rho_0^* \bar{w}\} - \\ & - \alpha \frac{\partial \dot{x}^3}{\partial z} \frac{\partial p_2}{\partial \dot{x}^3} + f' \rho_0^* (\bar{u} d' - \bar{v} d) - \bar{F}_3 \end{aligned} \quad (2c)$$

The symbols are explained in the Appendix. Compared to the nonrotated coordinate system the equations are modified by the rotation parameters $d = \sin \zeta$ and $d' = \cos \zeta$. For a system orientated in West-East and South-North direction the Eq. (2a-c) would result in the equations of motion used in common.

The subgrid-scale turbulent fluxes F_i are parameterized utilizing a first-order closure hypothesis. Below a height of 10 m above the ground, the validity of surface layer similarity theory is assumed for the calculation of the surface fluxes and exchange coefficients. Above that, the vertical exchange coefficients are determined after Dunst (1982) (see Schlünzen, 1990). The exchange coefficients depend linearly on the friction velocity and locally on atmospheric stability which is characterized by the local gradient Richardson number. It is a mixed-local-profile formulation.

It should be mentioned here that a fully local formulation for the exchange coefficient (eg. a turbulent kinetic energy, dissipation model) might be – at least theoretically – more adequate for modelling of steep terrain influences. However, not much is known on the parameterization of turbulent fluxes and exchange processes above topography and even the surface fluxes are unknown for uneven terrain. There are indications that the influence of uneven terrain on the turbulence structure may be small at least at higher altitudes (Mason and King, 1984) or for convective conditions (Krettenauer and Schumann, 1992). It might be sufficient to use the same formulation for the exchange coefficient for uneven terrain as for flat terrain.

2.2 Numerical Treatment and Boundary Conditions

The equations are solved on an ARAKAWA-C-grid with the components of the velocity vector

and several transformation coefficients (eg. $\partial \dot{x}^3 / \partial x, \partial \dot{x}^3 / \partial y$) staggered in space against scalar quantities. Advection and diffusion of momentum are calculated by use of the Adams-Bashforth scheme in time with centered differences in space. Pressure gradient forces are treated as implicit in time and centered in space. All other terms are solved forward in time and centered in space. The mesoscale pressure perturbation is calculated with the conjugate gradient method (Kapitza and Eppel, 1987). To suppress non-linear computational instability, a 7-point filter is used at each time step (Shapiro, 1971). Due to the necessary horizontal resolution of the model (see Section 3), the time step in the model calculations was limited to 2 seconds to prevent numerical instability.

A no-slip condition is used at the surface boundary resulting in vanishing components of the wind velocity vector. The components of surface fluxes depend on the friction velocity and the wind direction. The surface temperature is kept constant in the present model calculations. At the top of the model all vertical gradients are set to zero. At the lateral boundaries the boundary parallel components of the wind velocity vector are derived from zero flux assumptions. The normal components of the wind vector are calculated from the prognostic Eq. (2a-c) with the exception of boundary normal advection and diffusion. The boundary normal advection is calculated by use of radiation boundary conditions (Orlanski, 1976) at the upstream-boundary. At the downstream boundary an upstream advection scheme is used. The boundary normal diffusion is neglected.

2.3 Restrictions in Model Application for Steep Terrain

The coordinate transformation has been performed without neglect of any transformation terms in the equations (see Schlünzen, 1988, for details). Special care has been taken to ensure the physical conservation principles not only for the differential but also for the difference form of the equations. No simplifications or neglections have been made and the full equations have been discretized. Thus, the model should be appropriate for model studies not only over terrain with moderate but also with steep slopes. The theoretical limit of terrain slopes lies close to 90° , caused by the definiteness of the coordinate transformation (Eq. (1)).

Actually, the terrain slopes acceptable for a meso-scale model using terrain following coordinates might be much lower. Krettenauer and Schumann

(1992) name a limit of 45° for their model. In other papers the maximum slope is discussed in dependence on the applied numerical schemes (eg. Janjic, 1977; Mahrer, 1984; Adrian, 1987). It would thus seem to be useful to determine the maximum slope acceptable for the model METRAS from systematic model runs. The idealized 3-dimensional topography used for the model studies is given by:

$$z_s = H e^{-\{(x^2 - y^2)/L^2\}} \quad (3)$$

H is the height of the mountain and L the horizontal distance from the mountain top to a downstream point where the elevation is half its maximum. The parameters for several slopes are given in Table 1. The named slopes denote the maximum values. The model grid is uniform in horizontal direction in the area of the hill and increases towards the lateral boundaries.

The speed-up S calculated from the model results corresponds to a height of 10 m above ground. It is the normalized difference of the velocities in the influence area of the obstacle and in the undisturbed area close to the model boundaries.

$$S = \frac{|\mathbf{V}|_{\text{disturbed}} - |\mathbf{V}|_{\text{undisturbed}}}{|\mathbf{V}|_{\text{undisturbed}}} \cdot 100 \% \quad (4)$$

As can be seen from Table 1, the maximum speed-up increases up to about 130 % for a slope of 50° for steeper hills. For higher slopes the values remain about the same. This might be explained due to the more effective non-linear acceleration terms (Hunt and Simpson, 1982) and lee vortex generation for steeper terrain (see Figure 1). For moderate slopes (Figure 2) the horizontal cross section shows a flow above and around the mountain, a lee vortex is not generated.

The results from the systematic model runs have been compared with measurements (Geiger, 1961; Mason and Sykes, 1979; Taylor and Teunissen, 1987),

Table 1 Mountain height H and half width L , grid size, and calculated maximum speed-up S_{\max} for different terrain slopes

Maximum Slope	Hill characteristics				S_{\max} [%]
	H [m]	L [m]	Grid size [m]	H/L	
10°	500	2080	650	0.24	34
20°	500	975	300	0.5	68
30°	500	607	187	0.8	96
40°	500	416	128	1.2	113
50°	500	300	92	1.6	128
60°	500	200	62	2.5	132
70°	500	130	40	3.8	129

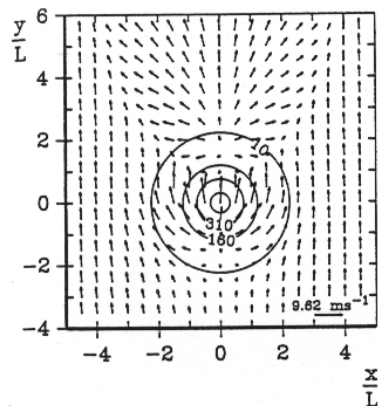


Figure 1 Horizontal cross section of the wind field 10 m above ground in the area of a mountain with maximum slopes of 60°; contours indicate height of the mountain.

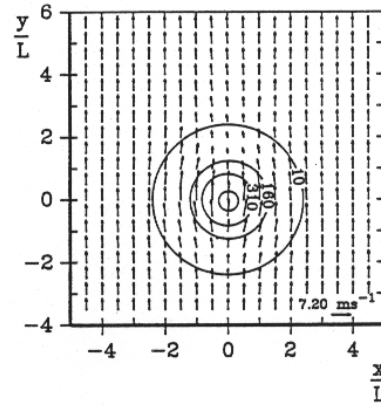


Figure 2 Same as Figure 1, but with maximum slopes of 20°.

Table 2 Values of the maximum speed-up S_{\max} determined in the height z from measurements, theory or model results

Hill characteristics							
Maximum Slope	H [m]	L [m]	H/L	Shape	S_{\max} [%]	z [m]	
14.4°	116	220	0.5	elliptic	110	3	Wind-tunnel simulations ¹
					80	10	
					40	50	
3° 10°	116	220	0.5	elliptic	60	10	Wind-tunnel simulations ²
					50	1.5	Measurement ³
18°	137	300	0.45	$\cos^2(x^2 + y^2)$	62	1.5	
					130	2	Measurement ⁴
					100		Theory ⁴
10°	300	1200	0.24	$e^{(x^2 + y^2)/a^2}$	50		Theory ⁵
					70	10	
					40		Model simulation ⁶

¹Teunissen et al. (1987) Wind-tunnel simulations of the Askervein A

²Teunissen et al. (1987) Wind-tunnel simulations of the Askervein AA

³Geiger (1961)

⁴Mason and Sykes (1979) Measurement at the Brent Knoll

⁵Hunt (1980)

⁶Gross and Etling (1984)

model results (Gross and Etling, 1984; Teunissen et al., 1987) and theory (Hunt, 1980; Hunt and Simpson, 1982; Jackson and Hunt, 1975; Taylor et al., 1987).

The values are compiled in Table 2. Some speed-up values calculated from measurements are much higher than the values calculated from our model results. Since the speed-up decreases with height (Table 2) volume mean values result in lower

numbers and the speed-ups lie in the same range as the model results.

The decrease of the speed up with height can also be seen in Figure 3. The horizontal profiles are calculated at 3 m and 10 m above ground from wind-tunnel experiments performed by Teunissen et al. (1987) for the Askervein. In Figure 4 the speed-up profiles are presented for our model results at a height of 10 m for maximum slopes of 10°, 20° and

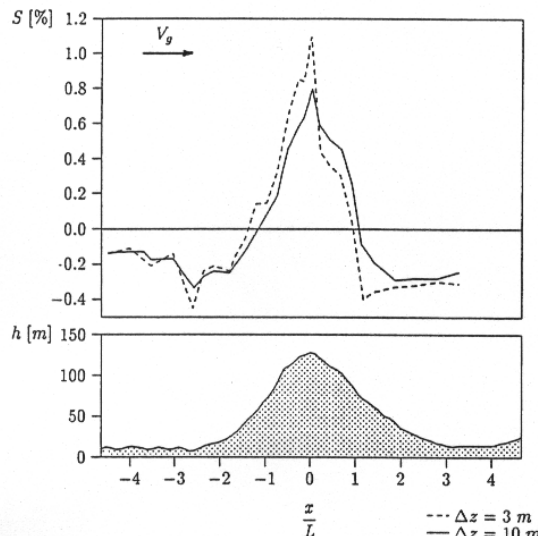


Figure 3 Top: Horizontal profile of the speed-up S at the Askervein for 3 and 10 m height above the ground. Bottom: The profile of the hill (after Teunissen et al., 1987).

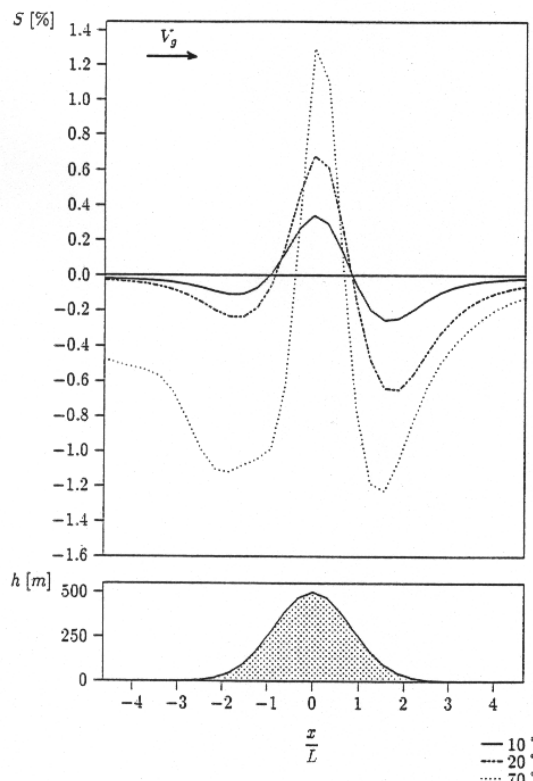


Figure 4 Horizontal profiles of the speed-up calculated from model results for a hill with maximum slopes of 10° , 20° and 70° .

70° . Both figures cannot be compared quantitatively due to the different shapes of the hills, the Askervein has an elliptical shape and the hill in the model a round one. Besides, the slope is at the windward side of the Askervein larger than on the lee side. But the figures can be compared qualitatively. The speed-ups are negative in windward and in lee side of the hill. The locations of the minima and maxima are in the same horizontal distance from the hilltop. Due to the elliptical shape of the Askervein the maximum of the speed-up (Figure 3) must be larger than for a circular shaped hill (Hunt, 1980) and larger than for the model result (Figure 4).

The model results show that the maximum speed-ups increase with the slopes (Figure 4 and Table 1) and decrease windward and in lee of the hill. The minimum is more intense at the lee than at the windward side. This agrees with measurements taken at the Brent Knoll (Mason and Sykes, 1979). For maximum slopes larger than 30° a vortex with a backward flow develops in lee of the hill. For slopes of 60° and 70° one develops at the windward side too.

Suitable data for comparison are restricted to moderate slopes. For steep terrain no data or other model results are available, and thus a comparison is not possible. Since the model results show a qualitative good agreement for moderate slopes and seem physically plausible for steep terrain we conclude that flow patterns up to a slope of 70° may be realistically simulated with model METRAS for neutral atmospheric stratification (see also Niemeier, 1992).

3 Modelling Area and Initialisation

The isle of Helgoland is located at $7^\circ 53'$ East and $54^\circ 10'$ North in the German Bight, about 70 km away from other islands and the mainland. For this reason, scientists are interested in measurements, taken on the island, representing the undisturbed conditions of more remote areas. Observations are taken, for example, by the German Weather Service (DWD) and by several meteorologists and chemists of the University of Hamburg at the observatory of the Department of Meteorology (MI).

To get an impression of Helgoland, its topography is briefly described. The island is divided into Oberland, Mittelland, Unterland and harbour area (Figure 5). The Oberland is a rock plateau that is 1200 m long, 50 to 300 m wide and up to 62 m high. The cliffs in the north and west of the island are nearly

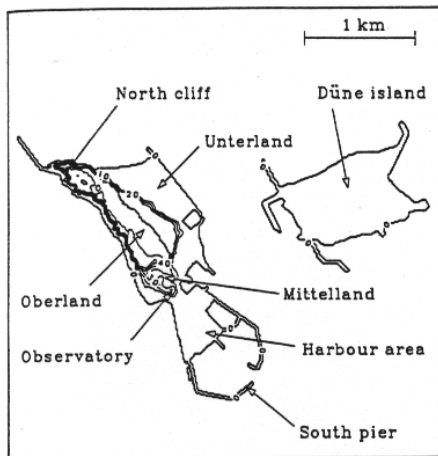


Figure 5 Topography of Helgoland and Düne island.

vertical. The east slopes are slanted by about 70° . Two craters characterize the Mittelland in the southeast which overviews the flat harbour area. The Unterland is a plain terrain east of the Oberland. In a distance of 1000 m east of Helgoland the sandy Düne island is located. It is only up to 6 m high and covers an area of $500 \times 700 \text{ m}^2$. The heavily built-up area of the village Helgoland is located at the east of the Oberland, the Unterland and the harbour area. The houses are three stories high. The other parts of the island, as well as the Düne island, are mainly covered with grass.

The surface characteristics are described in the model by nine different surface types (Table 3).

The observatory of the MI is situated on a hill in the Mittelland at a height of 20 m above sea level. It is a small building, its roof being at the same height as the top of the hill. The DWD has been operating several wind masts on the island in order to determine the influence of the island on the routine

Table 3 Roughness length z_0 for different surface types used in the simulations of flow patterns at the isle of Helgoland

Surface type	$z_0 [\text{m}]$
Water	0.000015
Sand	0.0003
Dune	0.04
Grass	0.01
Heath	0.05
Jetty	0.3
Bush	0.1
Low houses	0.5
Higher houses	0.7

measurements of wind velocity and direction. There are 15 m and 80 m high masts in the southern harbour area, a 10 m high one at the end of the south pier and another one in the middle of the Düne island (Schmidt, 1991). Previous routine measurements performed in the harbour area show a systematic error in the wind velocity for some wind directions (DWD, 1977).

The model runs have been initialized keeping the idea of generalization of the model results in mind. The general validity is only given when at least the following three questions can be positively answered:

1. Does the representation of the island in the model sufficiently reflect the realistic situation?
2. Are the results obtained with a wind velocity used in the model runs representative for other wind speeds?
3. Are the results obtained with a special atmospheric stability representative for other stratifications?

The first question will be answered with respect to the measurements in Section 4.4. The influences of different wind velocities can be characterized by use of the dimensionless Reynolds number. With a wind velocity larger than 1 ms^{-1} , the Reynolds number is large enough in the atmosphere and in the numerical simulations to result in turbulent flows. No changes in the flow patterns of the dimensionless speed-up can be expected for higher wind velocities. In the present simulations a geostrophic wind of 4.5 ms^{-1} has been prescribed. The used wind speed is in the lower range for the observed conditions at Helgoland but the interval of 0.3 to 5.4 ms^{-1} has a statistical frequency of 30 % (Table 5). Lower wind velocities are quite seldom and less relevant.

The atmospheric stability has an effect on the flow pattern around an obstacle. The effect depends on the obstacle, the wind velocity and the temperature gradient. It can be described by two different definitions of the dimensionless Froude number $F = |\mathbf{V}_g|/(N \cdot H)$ and $F_1 = |\mathbf{V}_g|/(N \cdot L)$. \mathbf{V}_g is the geostrophic wind velocity, N the Brunt-Väisälä frequency $N = (g/\theta_0 \cdot \partial\theta/\partial z)^{1/2}$, H the height of the obstacle and L the horizontal distance from the hill top to a point where the elevation is half its maximum. For F , $F_1 \rightarrow \infty$ the atmospheric stratification is neutral and for F , $F_1 \rightarrow 0$ very stable. Hosker (1984) describes the flow pattern around a three-dimensional hill measured by Hunt, Snyder and Lawson (1978) in a wind tunnel for several Froude numbers. He shows that for $F \geq 1.7$ the flow patterns

are similar to that of neutral stratification. Following Hunt and Simpson (1982), for this Froud number the streamlines are packed closer to the hilltop compared to neutral stratification, thus S will be slightly larger. Besides this the flow pattern shows no principle differences.

For $H = 50$ m, the height of Helgoland, $|V_g| = 4.5 \text{ ms}^{-1}$ and the potential temperature gradient $\partial\theta/\partial z = 0.35 \text{ K}/100 \text{ m}$, the Froud number results in $F = 8.0$. For a higher temperature gradient ($\partial\theta/\partial z = 1 \text{ K}/100 \text{ m}$) F becomes lower ($F = 4.8$). This is also true for a lower wind speed of 1.5 ms^{-1} ($F = 1.6$). The Froud number is 1.7 or less only for very stable stratification and a very low wind speed. Low wind speeds are very rare at Helgoland and very stable stratifications are also seldom. Therefore, the model simulations are performed with a neutral atmospheric stability. They are also representative for stable stratifications.

For the numerical simulations a geostrophic wind speed of 4.5 ms^{-1} has been prescribed in a neutrally stratified atmosphere. Since the island is not symmetric in any sense, different wind directions have been simulated. Eight simulations ($45^\circ, 90^\circ, \dots, 360^\circ$) were carried out. From the large-scale wind and stratification, balanced profiles of the wind are calculated with a 1-dimensional version of the model. These are used as initial values for the 3-dimensional model, in which the topography is introduced via diastrophism. All model results are averaged over one inertial oscillation (15 h) to reduce its influence on the horizontal wind components.

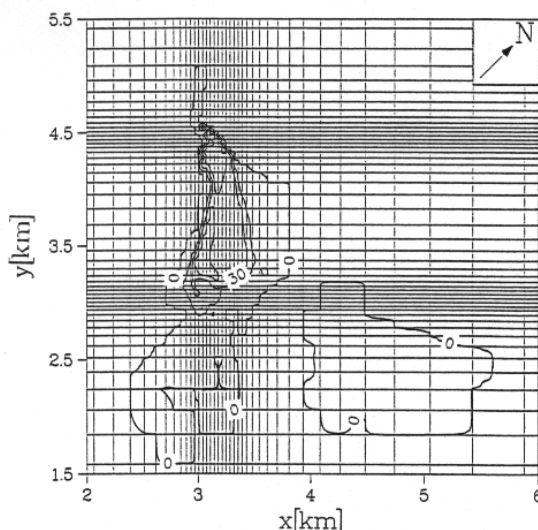


Figure 6 Inner part of the model area and grid structure.

For the model simulations it is necessary to interpolate the topography data on a model grid with the aim of a minimized number of grid points and a good resolution of the topography. For a good representation of the steep coast, directed from the northwest to the southeast, the model coordinate system is rotated 45° against North. Thus the y-direction of the grid is now parallel to the western coast (Figure 6) and with a minimum number of grid points a good horizontal resolution can be maintained. The grid has a horizontal mesh size of 35 m to 600 m and the resulting terrain slopes reach 45° to 55° which is low compared to the real values. A higher horizontal resolution and thus steeper coasts would increase the simulation requirements in an unacceptable way. For example, a minimum mesh size of 17 m and a maximal slope of 70° would quadruple the simulation time for the model. In the vertical direction the layers are also non-uniform with a grid size of 20 m close to the ground and 700 m at the model top at 7960 m.

4 Results

The influence of the isle of Helgoland on the flow patterns has been investigated by eight numerical simulations. The wind speed and the neutral stratification of the atmosphere are the same for each simulation, the wind direction is different. The wind directions named in this section correspond to the direction of the geostrophic wind in the non-rotated coordinate system.

The model results show differences in the flow patterns but also some similarities. Two individual results are presented in detail to describe very different situations (Section 4.1). A composite of all model results into a mean pattern shows the mean wind field (Section 4.2). A special interpretation of the results at the measurement sites elucidates the influence of the island on the wind measurements (Section 4.3). Finally the model results are compared with measurements (Section 4.4).

4.1 Calculated Flow Pattern for Different Wind Directions at the Isle of Helgoland

The performed simulations give insight into the changes of the undisturbed flow field due to the isle of Helgoland. All results show that upward winds develop at the windward side of the island and downward winds at the lee side. Areas with positive speed-ups always develop over the island and negative speed-ups at the windward and leeward

side. Different flow patterns are formed which are dependent on the geostrophic wind directions.

Geostrophic wind directions from north to southeast, for example, cause positive vertical velocities over the whole Oberland. For other directions the areas are much smaller. The largest differences from the undisturbed wind field are generated for a wind direction perpendicular to the longitudinal axis of the island. The influences are much smaller for a flow parallel to the coast. The obstacle is smaller and the flow goes more around the island. Additionally the enhanced roughness influences the flow pattern.

In the following sections the results for two wind directions are presented in more detail. Further results are shown in Niemeier (1992).

4.1.1 Northeast Wind

A geostrophic wind from the northeast hits nearly perpendicularly the eastern steep coast of Helgoland and produces positive and negative vertical winds at the windward and leeward side of the Oberland and Mittelland (Figure 7). The maximum upward motion (1.8 ms^{-1}) is located at the north cliff, the area of highest slopes. In the southeast direction the upward wind decreases to 0.6 ms^{-1}

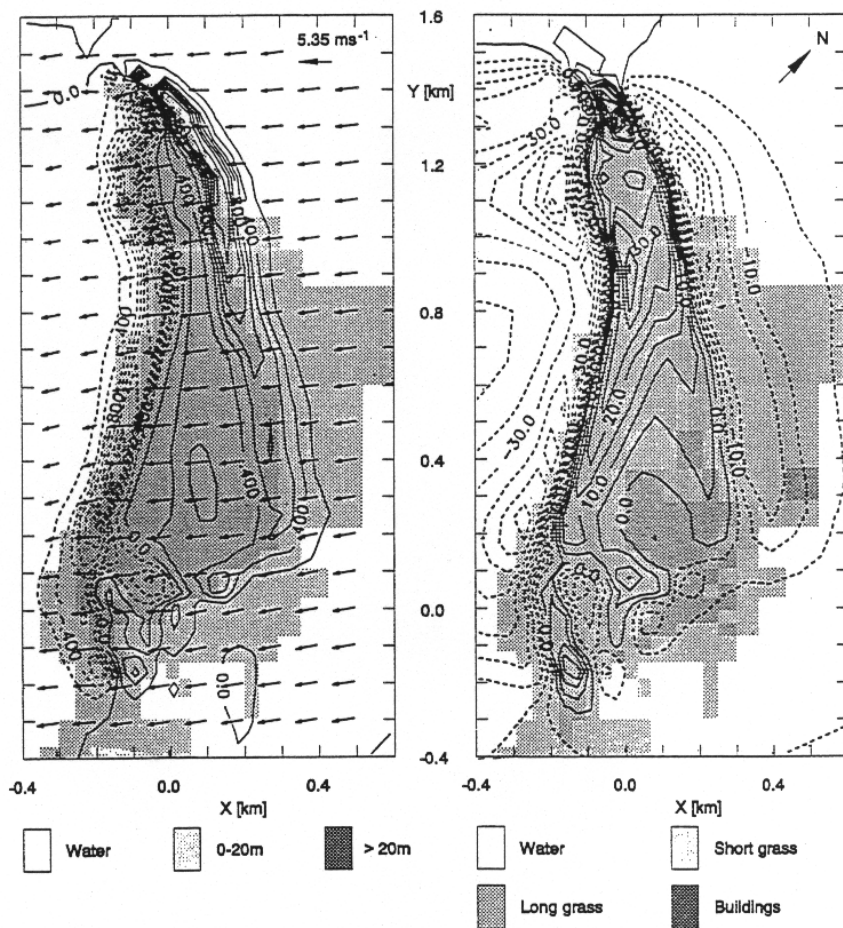


Figure 7 Model results for northeast wind and a velocity of 4.5 ms^{-1} . Left: wind vectors at 10 m and vertical velocity at 20 m above the ground (dashed contours indicate negative values, contour interval 0.2 ms^{-1}). The topography of Helgoland is shaded grey. Right: speed-up S [%] at 10 m above the ground (dashed contours indicate negative values, contour interval 5 %). The eight surface characteristics of the simulations are reduced to three characteristics shaded grey.

with decreasing slope. The downward winds are very regular along the western coast because the slope is quite similar. The small downward wind area in the lower part of the figure at the coordinate (0.2 km; -0.2 km) develops at a quay wall.

The speed-up (Figure 7, right) shows the influences of orography on the flow pattern, especially in the Mittelland. The areas of positive speed-up are at least 20 m above sea level. At the southern side of the crater (-0.15 km; -0.2 km) the velocity increases by up to 15 %. Further north, the other slope of the crater lies in lee of the Oberland and, thus, the velocity decreases. In the crater the wind velocity is 15 % lower than over the undisturbed sea. With the exception of the area of the village, the speed-up is positive all over the Oberland. A maximum speed-up of the horizontal velocity of

50 % develops at the north cliff and a minimum (-55 %) in lee of the western steep coast of the island.

4.1.2 Northwest Wind

A qualitatively and quantitatively different flow pattern results for northwest winds (Figure 8). In this case, the flow is parallel to the longitudinal axis of the island. The small obstacle produces extremely small disturbances, because the flow can stream around Helgoland more easily. This rotation of the wind can be seen from the wind vectors in the north. At this point a small upward wind area develops with a maximum of 1.2 ms^{-1} vertical velocity. A second one is visible in the south of the western steep coast. This local maximum has a vertical velocity of 0.8 ms^{-1} . At the transition from the

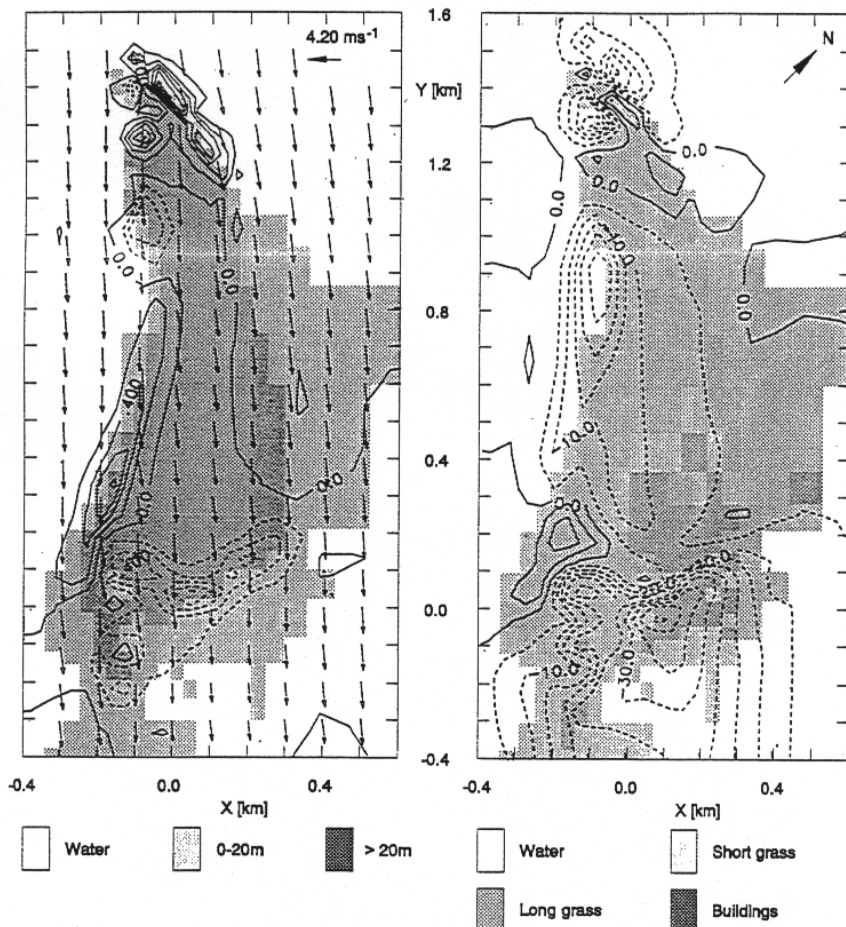


Figure 8 Model results for northwest wind, otherwise as in Figure 7.

Oberland to the Mittelland, the absolute maxima of downward winds are -0.8 ms^{-1} .

For northwest wind, the wind velocity is smaller than over the undisturbed sea nearly all over the island. At the north cliff a low positive speed-up of 5 % develops which occurs also in the south of the Oberland. There, the flow has to rise again due to topography. For this direction of flow the higher roughness over the island affects the wind velocity and causes a decreasing velocity. The reduction on the Oberland is -10% to -15% . On the windward and lee side of the north point the negative speed-up is -25% , and in lee of the Oberland the velocity decreases by up to -45% .

4.1.3 Survey of the Main Model Results

Altogether, Helgoland induces local structures in a horizontal homogeneous wind field. The maxima of the upward wind for the different wind directions are between 1.0 and 1.8 ms^{-1} and for the downward wind velocity between -1.0 to -2.2 ms^{-1} (Table 4). The maxima are mainly located at the north cliff, the area with the steepest slope. For a direction of flow parallel to the longitudinal axis of the island (southeast and northwest), the upward and downward winds are not as strong as for a direction of flow perpendicular (northeast and southwest).

The speed-up is lowest for wind directions from southeast and northwest. The absolute maxima of 50 % develops for wind directions from northeast and southwest and is located at the north cliff. For the cases with a direction of flow from southeast and northwest the maximum (10 %) is at the north cliff too. This indicates that the flow where the lower maximum occurs goes further around the island than the other one. Contrary to the wide range of values for the positive speed-up, the maxima of the negative speed-up only differ by 10 %. They are always located close to the island over the sea.

The influence of Helgoland on the wind direction is less than on the velocity. A gentle rotation develops

due to the higher roughness above the island or at the coastline compared to the wind direction at the same height over water. The consequences are limited to the area surrounding Helgoland. They do not extend as far out over the sea as do the deviations of the wind velocity. The maximum changes in wind direction are lower than 10° .

4.2 Mean Flow Pattern

The presented model results characterize the flow pattern for each wind direction separately. For planning measurement strategies it might be interesting to know the typical mean flow pattern. This is calculated by use of the weighted means of the results. Therefore, each result is multiplied by the statistical frequency of the wind direction and summed up for the mean flow pattern. The weighting factors are based on statistics for the distribution of wind with 10 min means of the years 1972 to 1976 (Table 5). The values are measured at a height of 10 m at a wind mast of the DWD. In the model results the named wind direction is the geostrophic one. The calculated ageostrophic angles lie between 10° and 20° over water. Therefore the wind statistics based on measurements is used as an approximation for the geostrophic wind directions. The statistics is summarized for all wind velocities and atmospheric stabilities.

According to the statistics, in 50 % of the cases the winds are coming from the direction between 225° (southwest) and 315° (northwest). Due to their frequency, the flow patterns for westerly wind have more influence on the results of the mean flow pattern and characterize them. This is clearly visible in the mean vertical wind field (Figure 9, left). The weighted mean of vertical velocities results in regular upward winds up to 0.3 ms^{-1} along the steep coast in the west. The absolute maximum is located in the middle part of the coast and a relative one at the north cliff. The downward winds are mainly very low. In the southeast part of the Oberland and in the

Table 4 Absolute extrema of vertical wind velocity and speed-up in the simulation results for the different wind directions

Wind direction	$w_{\min} [\text{ms}^{-1}]$	$w_{\max} [\text{ms}^{-1}]$	$S_{\min} [\%]$	$S_{\max} [\%]$
Northeast	-1.6	1.8	-55	50
East	-1.6	1.0	-50	25
Southeast	-1.0	1.0	-50	10
South	-2.2	1.6	-50	40
Southwest	-2.2	1.5	-55	50
West	-1.0	1.8	-45	30
Northwest	-1.0	1.2	-45	10
North	-1.4	1.8	-45	40

Table 5 Annual distribution of the measured wind velocity and direction frequency at the isle of Helgoland. The Table is based on values given by Duensing and Zöllner (1979)

Wind velocity [ms^{-1}]	0.3–5.4	5.5–10.7	10.8–17.1	> 17.2				
[%]	30.8	49.8	17.2	1.6				
Wind direction	45°	90°	135°	180°	225°	270°	315°	360°
[%]	8.0	11.9	10.4	10.3	15.3	17.5	15.3	10.4

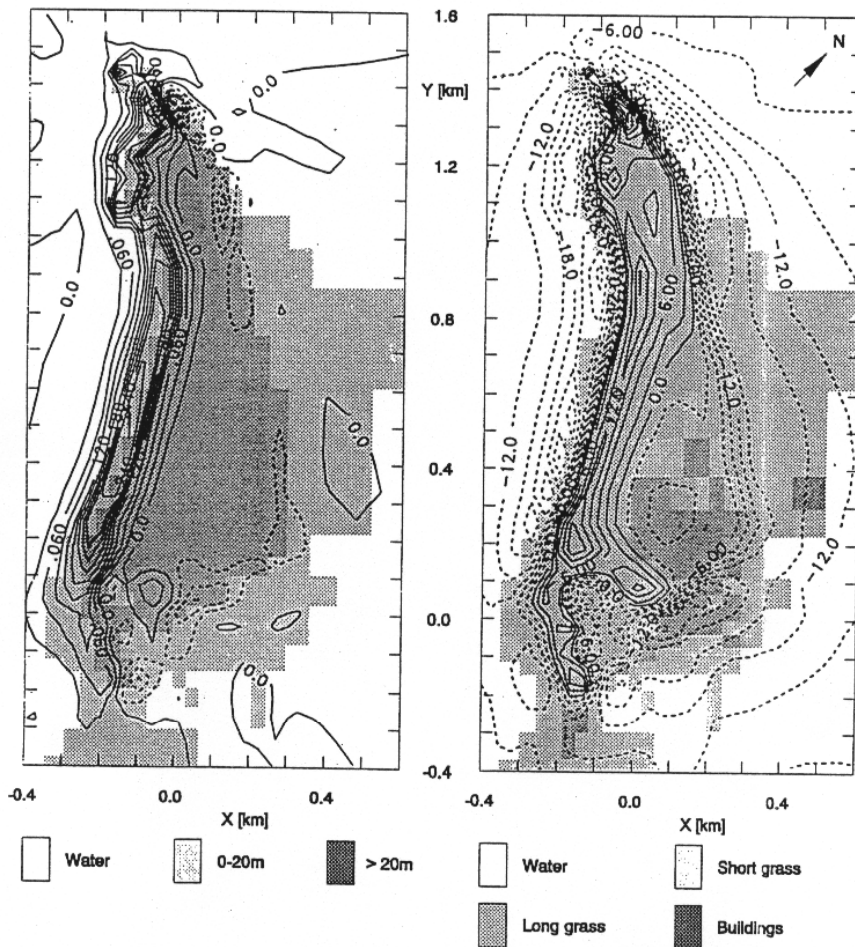


Figure 9 Mean flow pattern calculated from the single model results weighted by the wind direction frequency. Contour intervals are 0.03 ms^{-1} and 3 %, otherwise as in Figure 7.

Mittelland the local maximum is -0.09 ms^{-1} and the absolute one at the north cliffs is -0.21 ms^{-1} . The maximum vertical winds of the mean flow pattern make up only 10 % to 30 % of the individual results. All local effects are smoothed out.

The mean speed-up shows very well the increase of velocity over the Oberland (Figure 9, right). The maximum of 24 % is located at the north cliff. Along the western steep coast two local maxima develop with a speed-up of 15 %. On the slopes of the craters the velocity is decreasing by -15 % , around the Oberland -27 % , especially at the western steep coast and at the north cliff. In the area of the village on the Oberland, the velocities decrease by -6 % , and at the Unterland they decrease by -24 % .

The mean speed-up pattern shows more similarities to the individual results than the vertical wind fields

do. The maxima of mean speed-up values are only two times lower than the maxima of the individual results (Figure 7 and 8, right). The area of decreased velocity on the Oberland corresponds with the location of the village and is caused by it. The mean speed-up pattern is influenced by Helgoland and the Düne island in an area of 3 km around the Oberland (Figure not shown). At a distance of 1.5 to 2.5 km from the Oberland the mean velocity is decreased by a maximum of 3 % compared to the undisturbed sea. For an individual result it can be somewhat greater.

The mean flow pattern characterizes the areas on the island where the influence of Helgoland can be measured for all wind directions. However, if one is not interested in measuring the flow field around the island but wants to take area representative

measurements, the mean flow pattern is not sufficient. The individual model results have to be viewed with respect to measurement sites.

4.3 Interpretation of the Calculated Flow Patterns in Correspondence with Measurement Sites

For this interpretation, the modelled velocities at grid points over the undisturbed sea are compared with those at the points corresponding to measurement sites. The sites are the observatory of the MI and the wind masts of the DWD at the south pier, the southern harbour area, and the Düne island (Figure 5).

The vertical velocity is nearly zero at the measurement sites of the DWD. At the observatory it varies between -0.5 and 0.5 ms^{-1} with extrema for wind directions from east and west. The observatory itself is located at the eastern slope close below a hill top (see Figure 5). Therefore, upward winds occur for wind directions with an easterly component and downward winds for westerlies (Figure 10, left).

With a fixed large-scale wind velocity ($|V_g| = 4.5 \text{ ms}^{-1}$) the values of the speed-up vary for the different places by about 40 %. Noteworthy are the different results at the observatory with mostly positive speed-ups and at the three wind masts with exclusively negative speed-ups (Figure 10, right). These differences are caused by the location of the observatory on a hill in the Mittelland whereas the other sites are at lower ground.

Figure 11 shows calculated speed-up values at a height of 10 m for the different locations dependent on the geostrophic wind directions. In the speed-up roses the open bars correspond to negative speed-ups, a decreasing of the velocity compared to the values over the undisturbed sea. The full bars represent positive speed-ups, and the circles a velocity change of 10 %.

For a southwest wind the wind speed at the observatory is up to 25 % and for a northeast wind up to 19 % higher than the wind speed over the undisturbed sea (Figure 11). Lower speed-ups develop at a wind direction from southeast when the observatory is windward of the Oberland. Negative speed-ups (-7 to -9 %) result for wind directions from northwest to north with the observatory in lee of the Oberland.

The wind masts of the DWD are not located on a hill. Correspondingly, the velocity decelerating influences of the Oberland and of the enhanced roughness become more important. The velocities are reduced resulting in negative speed-ups. The influence of the obstacle decreases with increasing distance. Therefore, the less disturbed conditions can be expected the further away the measurement sites are from the Oberland.

The change in flow is minimal at the measurement site on the south pier (Figure 10 and Figure 11, most southern speed-up rose). The decreases in wind velocity windward of the Oberland have no effect for a southeast wind at the mast 1000 m away. The maximum difference is only 6 % and arises from

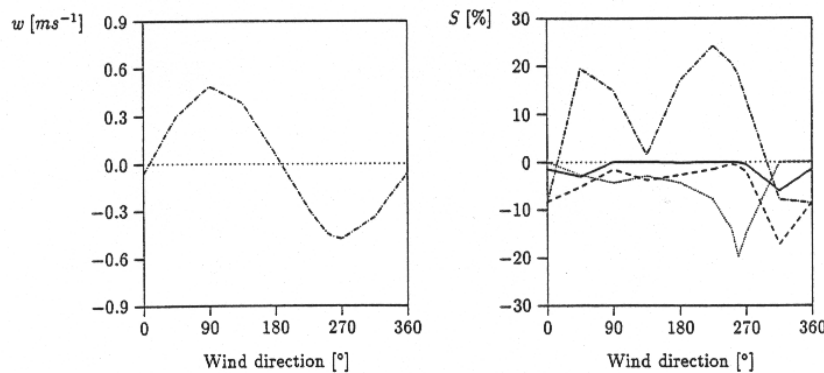


Figure 10 Simulated vertical wind velocity (left) and speed-ups (right) at the observatory (---) and at the wind masts of the DWD (Dünne island (· · ·), south pier (—), harbour area (— · —)) for the simulated geostrophic wind directions.

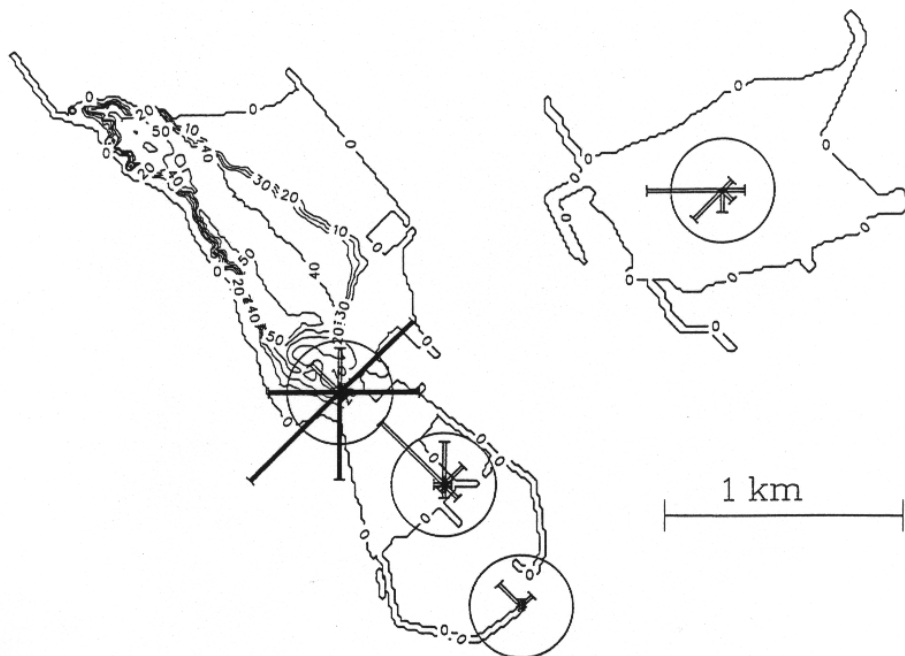


Figure 11 Simulated speed-up S at the observatory and at the wind masts of the DWD (Düne island, harbour area, south pier) for different wind directions. The open bars in the speed-up rose show negative speed-ups, the full bars positive speed-ups. The circles correspond to a velocity change of 10 %.

northwest winds when the measurement site is in the lee of the island. The velocity reduction is not as much as at each of the other measurement sites.

The measurement site at the Düne island is at a distance of 1400 m from the Oberland and is further away than the mast at the south pier. However, the Düne island is large enough to have an influence on the flow field too. For east wind the Düne island is windward of the Oberland and the negative speed-up is about -4 %. For westerly wind the Düne island is in lee of the Oberland. The maximum decrease of the velocity is -17 % for west wind. In this case the influences of the Oberland and roughness of the Düne island intensify each other, the disturbance is larger than at the south pier.

The curve of the speed-up for the mast at the harbour area is comparable to that for the mast at the south pier because the mast at the harbour area is located between the Oberland and the south pier. The lower distance to the Oberland results in a larger amplitude of the disturbances. For a wind direction from northwest the mast is in lee of the Oberland. The decreasing of the velocity is at the minimum with -17 %. For north wind it is still -8.5

%. A windward position of the mast results in a negative speed-up of -4 %.

Altogether the model results interpreted for the measurement sites harbour area, Düne island and south pier of the DWD show a lower influence when compared to the observatory. At the Düne island and the harbour area disturbances occur due to the influences of the lee. For other wind directions, the modifications of large-scale wind field due to the isle of Helgoland are relatively small. The site at the south pier might be a very good place for area representative meteorological measurements with only very small disturbances from the island. The largest difference of -6 % is very small compared to other sites at Helgoland.

The results for the measurement site observatory show large influences of Helgoland. If possible parameters which are dependent on the wind velocity should not be measured at this location. However, the wind direction is hardly influenced. Thus, measurements dependent on wind direction could be taken at the observatory as well as at other measurement sites on the island.

4.4 Comparison of Model Results and Measurements

The model results are compared to measurements taken at the wind masts of the DWD at Düne island, harbour area and south pier (Schmidt et al., 1993). The data presented in Figure 12 (left) are mean values for January 1990 to March 1992. A direct comparison of the measured and modelled data is impossible since the measurements include the climatology of the wind, e.g. lower wind speeds for northerly and southeast winds and higher velocities for southwest winds. The effect of the climatology overlaps the influence of the isle of Helgoland. As can be seen from Figure 12 (left) the measurements also include local effects. Otherwise, the three lines had to lie on top of each other. At the Düne island, for example, the velocities are lower for most wind directions than at the other measurement sites. This indicates that the island itself has an effect on the wind field. For easterly winds the velocities at the south pier (straight line) are relatively high. This is caused by local effects of the south pier which are not resolved in the model. If the direction of the flow is nearly perpendicular to the south pier, the wind velocity is enhanced and a positive speed-up of up to 12 % results (Schmidt et al., 1993). This effect is lower for high tide when the water-level is higher relative to the pier.

Since it is not possible to normalize the measured data with undisturbed wind speeds to calculate speed-up values, another comparative strategy is followed (see also Schmidt et al., 1993). Keeping in mind that the model results are representative for all meteorological situations (see Section 3) the calculated speed-ups are used to normalize the

measurements. If the model would include all local effects influencing the measurements the lines in Figure 12 (left) had to lie on top of each other. Figure 12 (right) shows the resultant wind velocities for the measurements at Düne island (dotted line), south pier (straight line) and harbour area (dashed line) for different wind directions. The correspondence is quite good for wind directions from southwest to north. For easterly winds the velocities at the south pier are higher compared to the other corrected measurements. As mentioned before the speed-up caused by the pier is not modelled. In this area the distance between two model grid points is too high to represent the small pier. Therefore, the model cannot calculate the positive speed-up at the south pier and the results must differ from each other. Another divergence in the corrected velocities exists for south and southeast winds. Here the model seems to underestimate the influences of the Düne island. The model grid might be too large to represent the hilly structures of the Düne island or the roughness used in the model is not as large as in the nature.

The comparison of uncorrected with corrected measurements (Figure 12) shows that the model results are good for the measurement site in the harbour area. Here the highest resolution in the model calculations has been used (Figure 6) and the main local effects can be modelled. Local influences are visible at the Düne island and at the south pier. They are not reproduced from the model. To determine the very local influences of the pier or of the dunes on the Düne island, the model grid must have a higher resolution in that areas. Besides these effects, the model calculations sufficiently reflect the realistic situation.

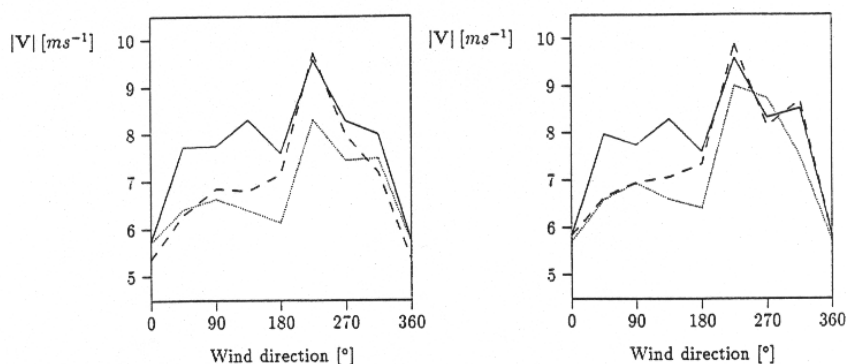


Figure 12 Data from the wind masts at the Düne island (···), the south pier (—) and the harbour area (---); uncorrected measurements (left) and measurements corrected with the model results (right).

5 Discussion and Conclusions

The presented model results show that a mesoscale model gives insight into the flow pattern over complex terrain. The simulations of the flow around hills of several slopes have shown that the model used, METRAS, can calculate the flow pattern over steep terrain with a maximum slope up to 70°.

The flow pattern at Helgoland has been calculated for different geostrophic wind directions and a neutral atmospheric stratification. The influences of the island on wind velocity are large for northeast and southwest winds and small for northwest and southeast winds, when the flow is perpendicular to the longitudinal axis of the island or parallel to this axis, respectively. The differences are caused by the elongated shape of the island. The vertical velocity differs in all cases between -2.2 and 1.8 ms⁻¹. The horizontal wind speed decreases -45 to -55 % at the windward and lee side of the island and increases at a maximum of 50 % over the island.

From the model results calculated for different geostrophic wind directions a characteristic mean flow pattern has been determined. As can be seen by comparison with individual flow patterns, the single wind field can be very different. From the mean flow pattern (Figure 9) areas can be found which are not suitable for wind velocity measurements for all geostrophic wind directions. Likewise, places on the island can be found where its influence on the flow pattern can always be measured. This might be interesting for further experimental strategies.

The results of the simulations are specifically analysed to determine the influences of the island on the measurement sites at the south pier, the Düne island, the harbour area and the observatory. The local influences are high at the observatory because of its location in the Mittelland. Here, the wind speed increases up to 25 %. At the Düne island and the harbour area the velocity decreases by -20 % due to the influences in lee of the island and the roughness. The simulation results show the lowest disturbances at a grid point corresponding to the measurement site at the south pier. Here, the influences of Helgoland on the large-scale wind field are lowest compared to the other sites. However, the comparison with measurements shows that the local influences for easterly winds are underestimated in the model calculations.

For a generalization of the model results only the speed-up values can be taken into account. The speed-up S is a dimensionless number and thus

describes qualitatively the resultant flow patterns and not their absolute values. In contrast the calculated vertical winds are dependent e.g. on the geostrophic wind velocity. Their values can not be generalized but are restricted to the present model calculations. In all simulations the geostrophic wind was constant at 4.5 ms⁻¹ and the vertical gradient of potential temperature was zero. This is a reduction of the real conditions in the atmosphere but it is sufficient to estimate the influence of the isle of Helgoland for neutral and stable atmospheric stratification as has been discussed in Section 3.

Finally, for a generalization of the model results the representation of the island in the model has to be sufficient to reflect the realistic situation. The cliffs are smoothed (45° to 55°) compared with reality (70° to 90°). However, as shown with the systematic model runs in Section 2.3 the speed-ups are only slightly enhanced for steeper terrain (see Table 1). In a simulation with a more realistic representation of the cliffs of Helgoland (maximum slopes between 60° and 70°), the calculated speed-up increases for 5 % and decreases in lee and downward for 15 % to 25 % (results shown in Niemeier, 1992). The comparison of uncorrected and corrected measurements has shown that the model resolution is mainly sufficient but not small enough at each site if all local effects should be modelled. The grid size would have to be reduced to a few meters only. This would result in an enormous increase in computer time unless a nested model would be used.

Altogether, the presented model results are sufficient to get an overall view of the behaviour of flows around the isle of Helgoland. The calculated speed-ups can be interpreted as values valid in general but they mark the lower limit of the possible speed-ups. The validity of the vertical winds is restricted to the presented case studies.

Acknowledgement

We would like to thank Mr. Schmidt and Mr. Pätsch from the Seewetteramt Hamburg (DWD) for making the topography and measurement data of Helgoland available to us and especially for the interesting discussions.

The detailed and helpful comments of two referees are appreciated.

This work was partly funded by the University of Hamburg and by the 'Bundesminister für Forschung und Technologie' under grant number MFU 0620/6.

Appendix

List of Main Symbols

d, d''	rotation parameters ($\sin \xi, \cos \xi$)
\bar{F}_i	divergence of subgrid-scale turbulent fluxes
f, f'	Coriolis parameter ($2\Omega \sin \varphi, 2\Omega \cos \varphi$)
g	acceleration due to gravity
H	height of an idealized mountain
L	half-width of an idealized mountain
p_1, p_2	mesoscale pressure (hydrostatic portion, dynamic portion)
S	speed-up
t	time
U_g, V_g	horizontal components of geostrophic wind vector in rectangular coordinates
\bar{u}, \bar{v}	horizontal components of wind vector in rectangular coordinates
$\bar{u}^i, i = 1, 2, 3$	contravariant components of wind vector $(\bar{u}(\partial \dot{x}^1 / \partial x), \bar{v}(\partial \dot{x}^2 / \partial y),$ $\bar{u}(\partial \dot{x}^3 / \partial x) + \bar{v}(\partial \dot{x}^3 / \partial y) + \bar{w}(\partial \dot{x}^3 / \partial z))$
\bar{w}	vertical wind
x, y, z	rectangular coordinate-system
$\bar{x}^i, i = 1, 2, 3$	terrain-following coordinate-system
z_s	height of topography above sea level in the rectangular coordinate-system
z_t	height of model top
$*\alpha$	grid volume
η	vertical coordinate in terrain-following coordinate-system
$\rho_0, \tilde{\rho}$	density of air (large-scale value, mesoscale value)
ϕ	latitude
ζ	rotation angle of coordinate-system
Ω	earth's angular velocity

References

- Adrian, G., 1987: Berechnung horizontaler Differenzen in geländefolgenden Koordinaten unter Berücksichtigung variabler vertikaler Gitterweiten, Meteorol. Rdsch **40**, 19–24.
- Avissar, R., and Y. Mahrer, 1988: Mapping frost sensitive areas with a three-dimensional local-scale numerical model. Part 2: Comparision with observations, Jour. of Appl. Met. **27**, 413–426.
- Bigalke, K., 1991: Interaktive Modellkopplung zur Berücksichtigung heißer Punktquellen in Gitterpunktsmodellen und Einfluß der Kopplungsstufe auf die Immission, 12, Berichte des ZMK. Meteorologisches Institut, Universität Hamburg, 141 pp.
- Clark, T. L., and R. Gall, 1982: Three-dimensional numerical model simulations of airflow over mountainous terrain: a comparision with observations, Mon. Wea. Rev., **110**, 766–791.
- DWD, 1977: Stationsbeschreibung Helgoland, 1 p.
- Duensing, G., and R. Zöllner, 1979: Die Windverhältnisse im Raum Helgoland unter besonderer Berücksichtigung der Windkraftnutzung, Einzelveröffentlichung 97, Deutscher Wetterdienst, Seewetteramt Hamburg, Hamburg, 61 pp.
- Dunst, M., 1982: On the vertical structure of the eddy diffusion coefficient in the PBL, Atmos. Env. **16**, 2071–2074.
- Geiger, R., 1961: Das Klima der bodennahen Luftsichten, Vieweg, Braunschweig, 423–436.
- Gross, G., and D. Etling, 1984: Mesoskalige Simulationsmodelle – ein Vergleich. Bericht für den Wissenschaftlichen Beirat des DWD, 17 pp.
- Hosker, R., 1984: Flow and diffusion near obstacles, in Atmospheric science and power production, United States Department of Energie. DOE/TIC – 27601, 241–426.
- Hunt, J., 1980: Wind over hills, in Workshop on the planetary boundary layer, J. Wyngaard, ed., American Met. Soc. Boston, 107–136.
- Hunt, J., and J. E. Simpson, 1982: Atmospheric boundary layers over non-homogeneous terrain, in Engineering Meteorology, E. J. Plate, ed., Amsterdam Elsevier, 269–318.
- Hunt, J., W. H. Snyder and R. E. Lawson, 1978: Flow structure and turbulent diffusion around a three-dimensional hill, in Fluid Modelling Study on Effects of Stratification, Part 1. Flow Structure, Report EPA-600/4-78-041.
- Jackson, P. and J. Hunt, 1975: Turbulent wind flow over low hills, Quart. J. R. Met. Soc. **101**, 929–955.
- Janjic, Z. I., 1982: Pressure gradient force and advection sheme used for forecasting with steep and small scale topography, Beitr. Phys. Atmosph. **50**, 186–199.
- Kapitza, H. and D. Eppel, 1987: A3-d. Poisson solver based on conjugate gradients compared to standart iterative methods and its performance on vector computers, J. Comp. Phys. **68**, 474–484.
- Krettenauer, K. and U. Schumann, 1992: Numerical simulation of turbulent convection over wavy terrain, J. Fluid Mech. **237**, 261–299.
- Mahrer, Y., 1984: An improved numerical approximation of the horizontal gradients in a terrain-following coordinate system, Mon. Wea. Rev. **112**, 918–922.
- Mason, P. and J. C. King, 1984: Atmospheric flow over a succession of nearly two-dimensional ridges and valleys, Quart. J. R. Met. Soc. **110**, 821–845.
- Mason, P. and R. Sykes, 1979: Flow over an isolated hill of moderate slope, Quart. J. R. Met. Soc. **105**, 383–395.

- Niemeier, U.*, 1992: Numerische Simulation von Strömungsfeldern im Bereich der Insel Helgoland, Diplomarbeit, Universität Hamburg, 84 pp.
- Orlanski, I.*, 1976: A simple boundary condition for unbounded hyperbolic flows, *J. Comp. Phys.* **21**, 251–269.
- Pielke, R. A.*, 1984: Mesoscale meteorological modelling, Academic Press, Orlando, 612 pp.
- Pielke, R. A.* and *Y. Mahrer*, 1978: Verification analysis of the University of Virginia three-dimensional mesoscale model – prediction over South Florida for 1 July, 1973, *Mon. Wea. Rev.* **106**, 1568–1589.
- Schlünzen, K. H.*, 1988: Das mesoskalige Transport- und Strömungsmodell 'METRAS' – Grundlagen, Validierung, Anwendung –, A 88, Hamburger Geophysikalische Einzelschriften, 139 pp.
- Schlünzen, K. H.*, 1990: Numerical studies on the inland penetration of sea breeze fronts at a coastline with tidally flooded mudflats, *Beitr. Phys. Atmosph.*, **63**, 243–256.
- Schlünzen, K. H.* and *U. Krell*, 1993: Mean and local transport in air, in circulation and contaminants fluxes in the North Sea, J. Sündermann, ed., Springer Verlag, Accepted for publication.
- Schlünzen, K. H.* and *S. Pahl*, 1992: Modification of dry deposition in a developing sea-breeze circulation – a numerical case study, *Atmos. Env.* **26A**, 51–61.
- Schmidt, H.*, 1991: private communication. Seewetteramt Hamburg.
- Schmidt, H.*, *J. Pätsch*, and *R. Strübing*, 1993: Ein begleitendes Windmeßprogramm auf der Insel Helgoland für die dort zu errichtende Windkraftanlage, Abschlußbericht BMFT-Projekt, in preparation.
- Schumann, U.*, *T. Hauf*, *H. Höller*, *H. Schmidt*, and *H. Volkert*, 1987: A mesoscale model for the simulation of turbulence, clouds, and flow over mountains: formulation and validation examples, *Beitr. Phys. Atmosph.*, **60**, 413–446.
- Shapiro, R.*, 1971: The use of linear filtering as a parametrization of diffusion, *J. Atm. Sci.* **28**, 523–531.
- Taylor, P.*, *P. Mason*, and *E. Bradley*, 1987: Boundary layer flow over low hills, *Boundary Layer Meteorology*, **39**, 107–132.
- Taylor, P.* and *H. Teunissen*, 1987: The Askervein Project: Overview and background data, *Boundary Layer Meteorology* **39**, 15–39.
- Teunissen, H.*, *M. Shokr*, *A. Bowen*, *C. Wood*, and *D. Green*, 1987: The Askervein Project: Wind-tunnel simulations at three length scales, *Boundary Layer Meteorology* **40**, 1–29.
- Wippermann, F.* and *G. Gross*, 1981: On the construction of orographically influenced wind roses for given distributions of the large-scale wind, *Beitr. Phys. Atmosph.* **54**, 492–501.